**SUPPORTING INFORMATION**

# Differential Ability of Five DNA Glycosylases to Recognize and Repair Damage on Nucleosomal DNA

Eric D. Olmon and Sarah Delaney*

Department of Chemistry, Brown University, Providence, Rhode Island 02912, United States

## Table of Contents

**Scheme S1**. DNA Sequences used in this study.

Nucleobase numbering is based on the crystal structure of Vasudevan, et al. [1]

Lesion-containing strand (Vasudevan strand "I")

5'- ATC AGA ATC CCG GTG CCG AGG CCG CTC AAT TGG TCG TAG ACA GCT
CTA GCA CCG CTT AAA CGC ACG TAC **X**$^{-3}$C**X**$^{-1}$ CT**X**$^{+2}$ TCC CCC GCG TTT
TAA CCG CCA AGG GGA TTA CTC CCT AGT CTC CAG GCA CGT GTC AGA
TAT ATA CAT CGA T -3'

Complement strand (Vasudevan strand "J")

5'- ATC GAT GTA TAT ATC TGA CAC GTG CCT GGA GAC TAG GGA GTA ATC
CCC TTG GCG GTT AAA ACG CGG GGG A**Y**$^{-2}$A G**Y**$^{+1}$G **Y**$^{+3}$GT ACG TGC GTT
TAA GCG GTG CTA GAG CTG TCT ACG ACC AAT TGA GCG GCC TCG GCA
CCG GGA TTC TGA T -3'

| **Duplex** | **X**$^{+2}$ | **Y**$^{-2}$ | **X**$^{-1}$ | **Y**$^{+1}$ | **X**$^{-3}$ | **Y**$^{+3}$ |
|---|---|---|---|---|---|---|
| **601** | G | C | G | C | G | C |
| **U**$^{OUT}$ | U | G | G | C | G | C |
| **U**$^{MID}$ | G | C | U | G | G | C |
| **U**$^{IN}$ | G | C | G | C | U | G |
| **8oxoG**$^{OUT}$ | 8-oxoG | C | G | C | G | C |
| **8oxoG**$^{MID}$ | G | C | 8-oxoG | C | G | C |
| **8oxoG**$^{IN}$ | G | C | G | C | 8-oxoG | C |
| **Hx**$^{OUT}$ | Hx | T | G | C | G | C |
| **Hx**$^{MID}$ | G | C | Hx | T | G | C |
| **Hx**$^{IN}$ | G | C | G | C | Hx | T |
| **εA**$^{OUT}$ | εA | T | G | C | G | C |
| **εA**$^{MID}$ | G | C | εA | T | G | C |
| **εA**$^{IN}$ | G | C | G | C | εA | T |
| **5OHU**$^{OUT}$ | 5-OHU | G | G | C | G | C |
| **5OHU**$^{MID}$ | G | C | 5-OHU | G | G | C |
| **5OHU**$^{IN}$ | G | C | G | C | 5-OHU | G |

**Figure S1**. Endonuclease III (EndoIII) reactivity.

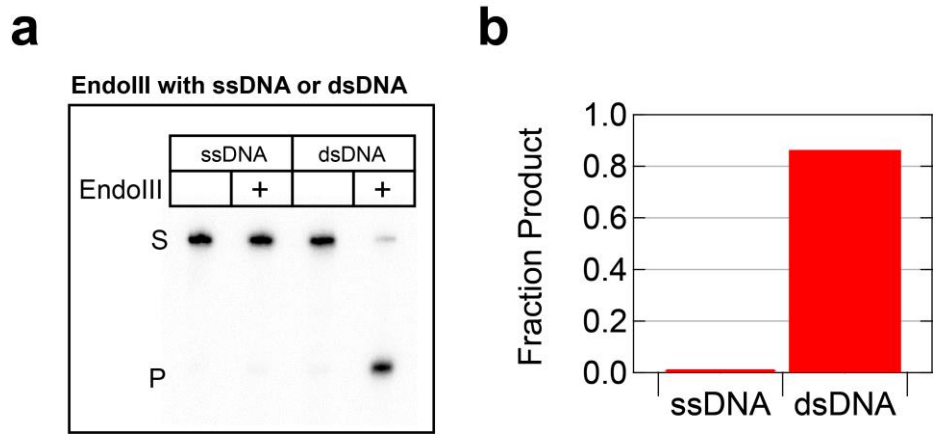


**Figure S1**. Endonuclease III (EndoIII) reactivity on single stranded (ssDNA) or double stranded (dsDNA) DNA substrates. (a) 8% denaturing polyacrylamide gel showing migration of an uncleaved substrate (S) or cleaved product (P) DNA strand. (b) Quantitation of product yield for samples including EndoIII. The data shown are the results of one trial.

**Figure S2**. Raw image of hydroxyl radical footprinting gel shown in Figure 2.

**Figure S2**. Raw image of hydroxyl radical footprinting gel shown in Figure 2. This gel image has not been straightened, cropped, or darkened. Lanes 6–10 are shown in Figure 2 of the main text.

**Figure S3**. Histograms of HRF damage.

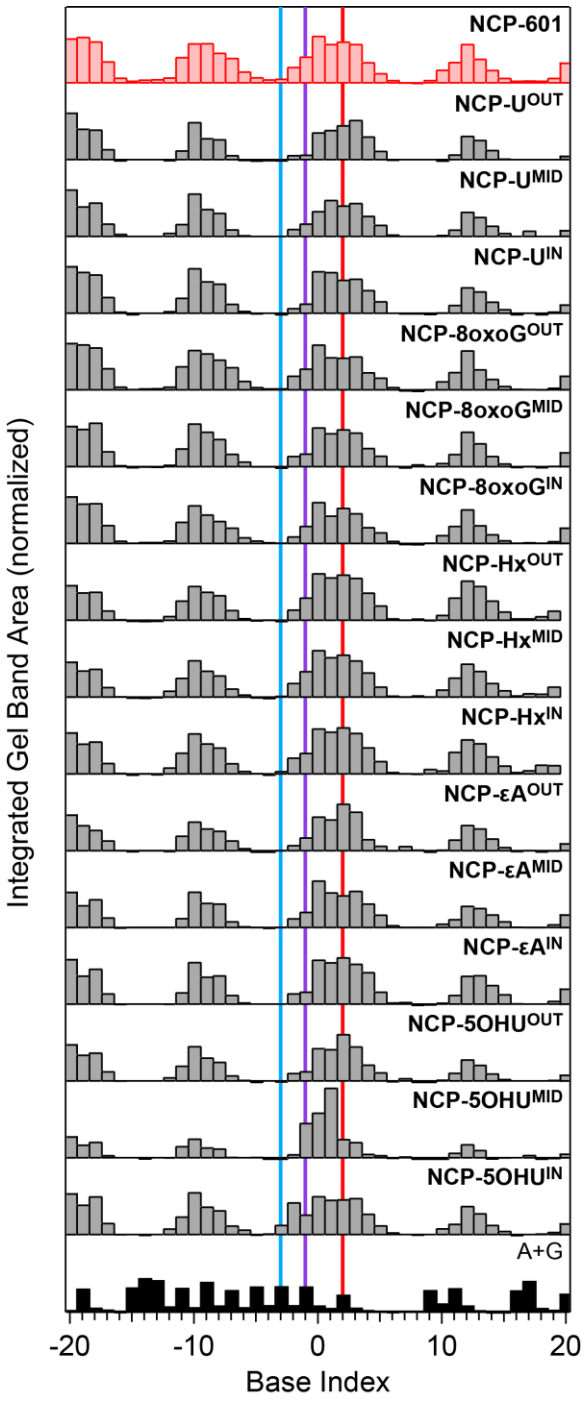


**Figure S3**. Histograms of HRF damage. Base positions indexed to the Vasudevan crystal structure. The OUT, MID, and IN positions indicated by red, purple, and blue lines, respectively. A+G denotes a Maxam-Gilbert sequencing lane. Excessive damage at positions –1, 0, and +1 of **NCP-5OHU$^{MID}$** is due to a small amount of incidental depyrimidination (~1%) at the lesion site, which partially obscures low intensity HRF damage.

**Figure S4**. Single turnover kinetics time courses.

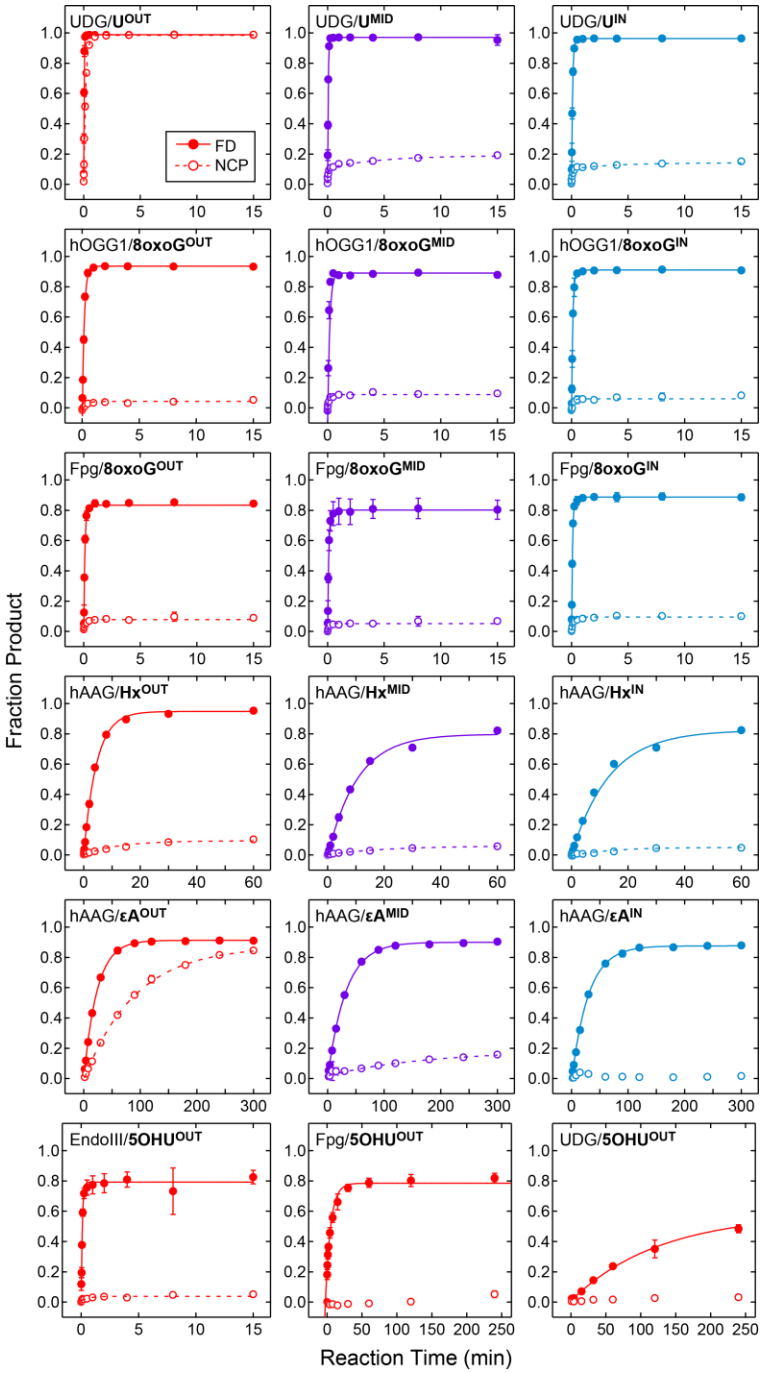


**Figure S4**. Single turnover kinetics time courses. Product formation is shown as a function of reaction time for glycosylases reacting on free duplex (closed circles) or NCP (open circles) substrates. Data were fit to the mean of three independent trials using nonlinear least-squares regression. Error bars represent the standard deviation.

**Figure S5**. Rate of Fpg and hAAG as a function of enzyme concentration.

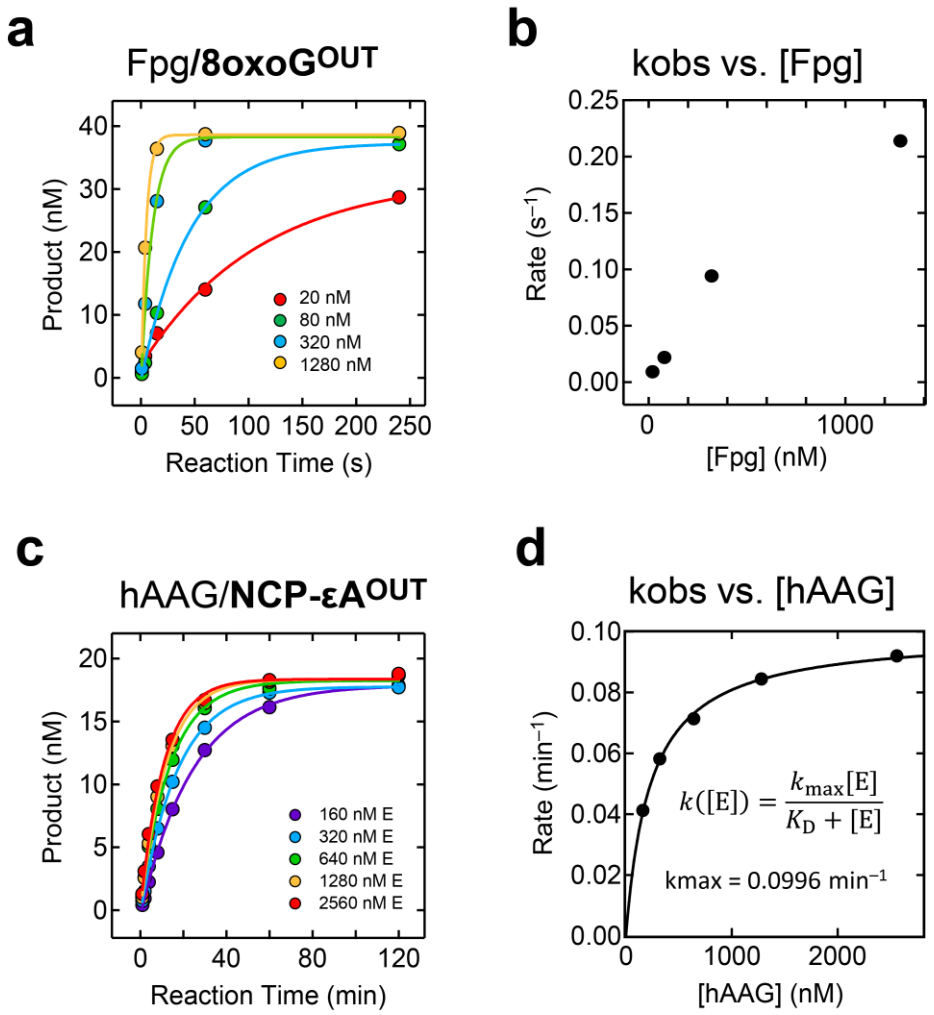


**Figure S5**. Rate of Fpg and hAAG as a function of enzyme concentration. (a) Product yield vs. reaction time for 40 nM **8oxoG$^{OUT}$** with 20, 80, 320, or 1280 nM Fpg. (b) Plots of $k_{obs}$ vs. [Fpg]. (c) Product yield vs. reaction time for 20 nM **NCP-εA$^{OUT}$** with 160, 320, 640, 1280, or 2560 nM hAAG. Plots of $k_{obs}$ vs. [hAAG]. Rate in STO reactions has been observed to change with [E] in many other systems, including topoisomerases,[2] restriction endonucleases,[3] and DNA glycosylases.[4–7]

**Figure S6**. A typical native gel showing NCP formation.

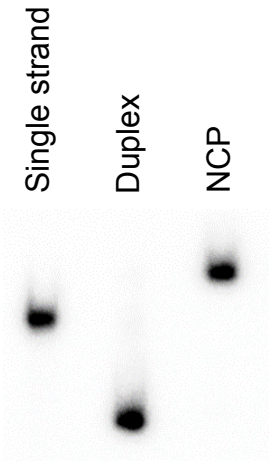


**Figure S6**. A typical native gel showing NCP formation. Radiolabeled samples were loaded onto a 1 mm thick, 7% native polyacrylamide gel (60:1 acrylamide:bisacrylamide, 0.25X TBE) and electrophoresed at 4 °C for 3 hours at 150 V in 0.25X TBE. Single stranded, duplex, and NCP DNA migrate differently.

**UDG Sequence Alignment**. Alignment of full-length and truncation human UNG with *E. coli* UDG.

Uniprot alignment using Genbank sequences 1296803 (Hsa UNG) and 148149 (Eco UDG)
NOTE: A truncation of 1296803 is used by Parikh, et. al. in *Proc. Natl. Acad. Sci. USA*, *97*(10), 5083–5088 (2000).

```
>gi|1296803|emb|CAA61579.1| uracil-DNA-glycosylase, UNG1 [Homo sapiens]
MGVFCLGPWGLGRKLRTPGKGPLQLLSRLCGDHLQAIPAKKAPAGQEEPGTPPSSPLSAEQLDRIQRNKA
AALLRLAARNVPVGFGESWKKHLSGEFGKPYFIKLMGFVAEERKHYTVYPPPHQVFTWTQMCDIKDVKVV
ILGQDPYHGPNQAHGLCFSVQRPVPPPPSLENIYKELSTDIEDFVHPGHGDLSGWAKQGVLLLNAVLTVR
AHQANSHKERGWEQFTDAVVSWLNQNSNGLVFLLWGSYAQKKGSAIDRKRHHVLQTAHPSPLSVYRGFFG
CRHFSKTNELLQKSGKKPIDWKEL

>gi|148149|gb|AAA24743.1| uracil DNA glycosylase [Escherichia coli]
MANELTWHDVLAEEKQQPYFLNTLQTVASERQSGVTIYPPQKDVFNAFRFTELGDVKVVILGQDPYHGPG
QAHGLAFSVRPGIAIPPSLLNMYKELENTIPGFTRPNHGYLESWARQGVLLLNTVLTVRAGQAHSHASLG
WETFTDKVISLINQHREGVVFLLWGSHAQKKGAIIDKQRHHVLKAPHPSPLSAHRGFFGCNHFVLANQWL
EQRGETPIDWMPVLPAESE

CLUSTAL O(1.2.2) multiple sequence alignment

uracil-DNA-glycosylase, mgvfclgpwglgrklrtpgkgplqllsrlcgdhlqaipakkapagqeepgtppssplsae 60
uracil                  ------------------------------------------------------------


uracil-DNA-glycosylase, qldriqrnkaaallrlaarnvpvgfgeswkkhlsgefgkpyfiklmgfvaeer-khytvy 119
uracil                  ----------------------maneltwhdvlaeekqqpyflntlqtvaserqsgvtiy 38
                                              :.   :*:. *: *  :***:: :  **.** .  *:*

uracil-DNA-glycosylase, ppphqvftwtqmcdikdvkvvilgqdpyhgpnqahglcfsvqrpvppppsleniykelst 179
uracil                  ppqkdvfnafrftelgdvkvvilgqdpyhgpgqahglafsvrpgiaippsllnmykelen 98
                        ** ::**.  :: :: *************** *****.***:  :  **** *:****..

uracil-DNA-glycosylase, diedfvhpghgdlsgwakqgvlllnavltvrahqanshkergweqftdavvswlnqnsng 239
uracil                  tipgftrpnhgyleswarqgvlllntvltvragqahshaslgwetftdkvislinqhreg 158
                         *  *.:* ** *..**:*******:****** **.** . *** *** *:* :**. :*

uracil-DNA-glycosylase, lvfllwgsyaqkkgsaidrkrhhvlqtahpsplsvyrgffgcrhfsktnellqksgkkpi 299
uracil                  vvfllwgshaqkkgaiidkqrhhvlkaphpsplsahrgffgcnhfvlanqwleqrgetpi 218
                        :*******:*****: **::*****:: ******.:******.**  :*: *:: *:.**

uracil-DNA-glycosylase, dwkel------ 304
uracil                  dwmpvlpaese 229
                        **  :
```

Truncation used in Parikh, et al.:

```
>1EMH:A|PDBID|CHAIN|SEQUENCEMEFFGESWKKHLSGEFGKPYFIKLMGFVAEERKHYTVYPPPH
QVFTWTQMCDIKDVKVVILGQDPYHGPNQAHGLCFSVQRPVPPPPSLENIYKELSTDIEDFVHPGHGDLS
GWAKQGVLLLNAVLTVRAHQANSHKERGWEQFTDAVVSWLNQNSNGLVFLLWGSYAQKKGSAIDRKRHHV
LQTAHPSPLSVYRGFFGCRHFSKTNELLQKSGKKPIDWKEL

CLUSTAL O(1.2.2) multiple sequence alignment

1EMH:A|PDBID|CHAIN|SEQUENCE      MEFFGESWKKHLSGEFGKPYFIKLMGFVAEER-KHYTVYPPPHQVFTWTQMCDIKDVKVV   59
gi|148149|gb|AAA24743.1|         -MANELTWHDVLAEEKQQPYFLNTLQTVASERQSGVTIYPPQKDVFNAFRFTELGDVKVV   59
                                       :*:. *: *  :***:: :  **.** .  *:*** ::**.  :: :: *****

1EMH:A|PDBID|CHAIN|SEQUENCE      ILGQDPYHGPNQAHGLCFSVQRPVPPPPSLENIYKELSTDIEDFVHPGHGDLSGWAKQGV   119
gi|148149|gb|AAA24743.1|         ILGQDPYHGPGQAHGLAFSVRPGIAIPPSLLNMYKELENTIPGFTRPNHGYLESWARQGV   119
                                 ********** *****.***:  :  **** *:****.. *  *.:* ** *..**:***

1EMH:A|PDBID|CHAIN|SEQUENCE      LLLNAVLTVRAHQANSHKERGWEQFTDAVVSWLNQNSNGLVFLLWGSYAQKKGSAIDRKR   179
gi|148149|gb|AAA24743.1|         LLLNTVLTVRAGQAHSHASLGWETFTDKVISLINQHREGVVFLLWGSHAQKKGAIIDKQR   179
                                 ****:****** **.** . *** *** *:* :**. :*:*******:*****: **::*

1EMH:A|PDBID|CHAIN|SEQUENCE      HHVLQTAHPSPLSVYRGFFGCRHFSKTNELLQKSGKKPIDWKEL------     223
gi|148149|gb|AAA24743.1|         HHVLKAPHPSPLSAHRGFFGCNHFVLANQWLEQRGETPIDWMPVLPAESE     229
                                 ****:: ******.:******.**  :*: *:: *:.****  :
```

# MATERIALS AND METHODS

**Oligonucleotide Synthesis and Purification**. DNA strands were synthesized on a MerMaid 4 oligonucleotide synthesizer (BioAutomation) using phosphoramidite chemistry. All phosphoramidites and reagents for DNA synthesis were purchased from Glen Research. Incorporation of noncanonical nucleotides and oligonucleotide deprotection were carried out according to protocols from Glen Research. For oligonucleotides containing 8-oxoG, the trityl group was removed during synthesis. Oligonucleotides containing 8-oxoG were purified by anion exchange HPLC (Dionex DNAPac PA100 anion-exchange column; A = 10% acetonitrile, B = 0.8 M ammonium acetate in 10% acetonitrile; 70:30 to 0:100 A:B over 35 min at 1 mL/min) and desalted by buffer exchange using centrifugal concentrators (Sartorius Vivaspin Turbo 15, 5 kDa MWCO). For all other oligonucleotides, the trityl group was retained during an initial round of purification by reversed-phase HPLC (Dynamax Microsorb C18 column, 10 × 250 mm; A = acetonitrile, B = 30 mM ammonium acetate; 5:95 to 35:65 A:B over 30 min at 3.5 mL/min). Samples were detritylated by incubation for 60 min at ambient temperature in 20% v/v aqueous glacial acetic acid, and then purified by reversed-phase HPLC at 90 °C (oligonucleotides containing only canonical bases and U) or 70 °C (oligonucleotides containing εA or 5-OHU) (Agilent PLRP-S column, 250 mm × 4.6 mm; A = 100 mM triethylammonium acetate [TEAA] in 5% aqueous MeCN, B = 100 mM TEAA in MeCN; 0:100 to 15:85 A:B over 35 min, 15:85 to 35:65 A:B over 5 min at 1 mL/min).

**Ligation to Form 145-mer Oligonucleotides**. Full-length 145-mer oligonucleotides were prepared by enzymatic ligation. First, component oligonucleotides were phosphorylated in the presence of 2 mM ATP using T4 polynucleotide kinase (New England Biolabs). Next, phosphorylated component oligonucleotides were combined with complementary scaffold oligonucleotides at a ratio of 1:0.95. The component strands were annealed to the scaffold strands by incubation at 90 °C for 5 min followed by cooling to 25 °C at a rate of 1 °C/min. Finally, the component strands were ligated by incubation with T4 DNA ligase (New England Biolabs; 400 units/nmol ligation sites) for 2 hrs at ambient temperature. Ligation products were purified by reversed-phase HPLC (Agilent PLRP-S column, 250 mm × 4.6 mm; A = 0.1 M TEAA in MeCN, B = 0.1 M TEAA in 1% v/v MeCN; 0:100 to 10:90 A:B in 10 min, 10:90 to 15:85 A:B in 40 min at 1 mL/min) or by 8% polyacrylamide gel electrophoresis (PAGE). Product identities were confirmed by electrospray ionization-mass spectrometry. Oligonucleotide concentrations were determined by their absorbance at 260 nm using molar extinction coefficients calculated using OligoAnalyzer 3.1 (www.idtdna.com). Final yields for 10 nmol scale ligations were 15–30%.

**Glycosylase Expression and Purification**. $His_6$-tagged hOGG1 was prepared recombinantly from *E. coli* as previously described.[8] The enzyme was purified by Ni-NTA affinity chromatography (GE Healthcare HisTrap HP, 5 mL), cation exchange chromatography (GE Healthcare HiTrap Q HP, 1 mL) and anion exchange chromatography (GE Healthcare HiTrap SP HP, 5 mL). Pure fractions were combined, concentrated (Amicon Ultra-15 centrifugal concentrator, 30 kDa MWCO), and resuspended in storage buffer (20 mM Tris-HCl [pH 7.5], 100 mM KCl, 10 mM 2-mercaptoethanol, 50% v/v glycerol). Aliquots of 0.5 mL were flash frozen in liquid nitrogen and stored at –80 °C until use. Analysis by SDS-PAGE showed the protein to be > 98% pure. UDG, Fpg, and hAAG were purchased from New England Biolabs. EndoIII was a kind gift from the laboratory of Jacqueline K. Barton (California Institute of Technology). The total concentration of each enzyme was determined by the Bradford method using a γ-globulin standard (Bio-Rad Laboratories).

**Reconstitution of Nucleosome Core Particles**. Recombinant expression and purification of histone proteins from *X. laevis* and refolding of the histone octamer were performed according to the standard method of Luger, et al.[9,10] NCPs were reconstituted by stepwise dialysis in a manner similar to that of Ye, et al.[4] Specifically, histone octamer was added to 100 µl of 1 µM duplex DNA in buffer (10 mM Tris-HCl [pH 7.5], 1 mM EDTA, 1 mM dithiothreitol [DTT], 2 M NaCl) at a mole ratio of 1.05:1. The mixture was

transferred to a Slide-a-Lyzer dialysis device (0.1 mL capacity, 3.5 kDa MWCO; Thermo Fisher Scientific), and the dialysis device was placed into buffer (10 mM Tris-HCl [pH 7.5], 1 mM EDTA, 1 mM DTT, 2 M NaCl) at 4 °C. At 60 min intervals, the dialysis buffer was replaced with analogous buffers containing successively lower concentrations of NaCl (1.2 M, 1.0 M, 0.6 M, 0 M). The final dialysis step was carried out for 3 hrs. Following dialysis, mixtures were filtered to remove precipitates. NCP formation was confirmed by 7% native polyacrylamide (60:1 acrylamide:bisacrylamide; 0.25X TBE) gel electrophoresis (3 h at 150 V, 4 °C). A typical native gel is shown in Figure S6.

**Hydroxyl Radical Footprinting**. Hydroxyl radical footprinting (HRF) was carried out using a variation of the method of Tullius.[11,12] Briefly, 7.5 µl of each 10 mM Fe(II)-EDTA, 10 mM sodium ascorbate, and 0.12% w/v aqueous hydrogen peroxide were combined with 10 pmol NCPs containing $^{32}$P-end-labeled DNA in 52.5 µL buffer (10 mM Tris-HCl [pH 7.5], 1 mM EDTA). The mixture was incubated at ambient temperature for 5 min, and then the reaction was quenched with the addition of 10 µL 1 mM EDTA in 25% v/v glycerol. The sample was immediately applied to a 5% native polyacrylamide (60:1 acrylamide:bisacrylamide; 0.25X TBE) gel, and NCPs were resolved from unbound DNA by electrophoresis (3 h at 150 V, 4 °C). Gel bands containing NCPs were incised, and NCPs were eluted into buffer (300 mM sodium acetate [pH 8.0], 1 mM EDTA) overnight. The solution was concentrated using a centrifugal concentrator (Sartorius Vivaspin Turbo 15, 5 kDa MWCO) and filtered. The sample was extracted against 25:24:1 phenol:chloroform:isoamyl alcohol, and the resulting aqueous phase was concentrated by rotary evaporation. Following addition of 20 µL co-precipitation agent (0.5 mg/ml tRNA in 300 mM sodium acetate [pH 8.0], 1 mM EDTA), samples were desalted by ethanol precipitation. Cleavage fragments were resolved by 8% denaturing PAGE and imaged by phosphorimagery. Fragment bands were quantitated using SAFA gel analysis software.[13]

**Glycosylase Kinetics Experiments**. An alkaline cleavage assay was used to quantify the fraction of product formed in glycosylase assays.[8,14] In each system, the lesion-containing DNA strand was 5′-end labeled with [γ-$^{32}$P]-ATP. All glycosylase experiments were conducted at 37 °C with 20 nM substrate and sufficient enzyme to achieve single turnover conditions (640 nM UDG, hOGG1, hAAG, EndoIII; 1280 nM Fpg). For all experiments, substrate and enzyme stocks were prepared at 2X experimental concentration in reaction buffer (20 mM Tris-HCl [pH 7.6], 50 mM NaCl, 150 mM KCl, 1 mM EDTA, 1 mM DTT, 200 µg/ml BSA). In general, time courses were conducted by combining equal volumes of substrate and enzyme stocks, allowing them to react for varying amounts of time, and then quenching the reaction by adding NaOH.

Depending on the duration of the time course, one of two detailed experimental protocols was followed. Protocol 1: for time courses of 15 min or less (UDG/U, hOGG1/8-oxoG, Fpg/8-oxoG, hAAG/Hx, EndoIII/5-OHU), the substrate stock was divided into samples of 8 µl each. Following temperature equilibration (2 min at 37 °C), 8 µl enzyme stock was added to the substrate sample. After a variable reaction time, the reaction was quenched with the addition of 16 µl 1 M NaOH (U, 8-oxoG, Hx) or 32 µL 0.3 M NaOH (εA, 5-OHU). Protocol 2: for time courses longer than 15 min (hAAG/εA, UDG/5-OHU, Fpg/5-OHU), the temperature-equilibrated substrate and enzyme stocks were mixed. At each time point, 16 µL was removed from the reaction mixture and quenched by combining it with 16 µL 1 M NaOH (U, 8-oxoG, Hx) or 32 µl 0.3 M NaOH (εA, 5-OHU).

For each time course, a negative control (–C) sample was prepared by incubating 8 µl of substrate at 37 °C for the duration of the time course, adding NaOH, and then adding 8 µl enzyme. In the –C samples, the presence of NaOH prevents glycosylase activity, but any pre-existing damage, or incidental damage that occurs as a result of sample work-up, is exposed. Such damage is generally less than 5%.

After quenching, sample manipulation was the same for all experiments. Samples were heated for 2 min at 90 °C (U, 8-oxoG, Hx) or 12 min at 70 °C (εA, 5-OHU) to induce strand cleavage at abasic sites and to convert β-elimination products to δ-elimination products.[15] DNA was isolated from NCP samples by extraction against 25:24:1 phenol:chloroform:isoamyl alcohol. All samples were treated with 20 µl co-precipitation agent (0.5 mg/ml tRNA in 300 mM sodium acetate [pH 8.0], 1 mM EDTA) and desalted by

ethanol precipitation. Products were resolved by 8% denaturing PAGE, imaged by phosphorimagery (Bio-Rad PharosFX), and quantitated by densitometry (Bio-Rad Quantity One).

The fraction of product at each time point, $F_P(t)$, was determined by the formula

$$F_P(t) = \frac{\delta_P(t)}{\delta_S(t) + \delta_P(t)}$$

where $\delta_S(t)$ and $\delta_P(t)$ are the densities of the substrate and product gel bands, respectively, at time $t$. The time-dependent product yield, $P(t)$, was corrected for pre-existing and incidental substrate damage using the following formula:

$$P(t) = \frac{F_P(t) - F_P(0)}{1 - F_P(0)}$$

where $F_P(0)$ is the fraction of product observed in the –C sample. The mean product yield from three independent trials was determined at each time point. The averaged data were fit to the modified first-order integrated rate law:

$$[P(t)] = [P(\infty)]\left(1 - e^{-k_{obs}t}\right) + [P(0)]$$

or

$$[P(t)] = [P_1(\infty)]\left(1 - e^{-k_{obs,1}t}\right) + [P_2(\infty)]\left(1 - e^{-k_{obs,2}t}\right) + [P(0)]$$

where $[P(t)]$ is the concentration of product at time $t$, $[P(\infty)]$ is the maximum concentration of product, and $[P(0)]$ is the amount of product at time $t$ = 0 (generally close to zero), using weighted (standard deviation) nonlinear least squares regression (Wavemetrics IGOR Pro). Reaction rates, $k_{obs}$, were extracted from the fits.

**Molecular Modeling**. Molecular models were generated to visualize DNA glycosylase binding on NCPs. Initial structures of glycosylase-bound NCPs were prepared by aligning crystal structures of DNA-bound glycosylases hUNG (PDB ID: 1EMH, resolution: 1.8 Å), hOGG1 (PDB ID: 1EBM, resolution: 2.1 Å), Fpg (PDB ID: 1K82, resolution: 2.1 Å), hAAG (PDB ID: 1EWN, resolution: 2.1 Å), and EndoIII (PDB ID: 1P59, resolution: 2.5 Å) with the NCP crystal structure of Vasudevan, et al.[1] (PDB ID: 3LZ0, resolution: 2.5 Å) using the molecular graphics and modeling package PyMOL.[16] To perform the alignment, the phosphate atoms of the three base pairs on either side of the lesion in each glycosylase structure were aligned with the phosphate atoms of the three base pairs on either side of the "+02" position of DNA strand "I" in the NCP structure using the "pair_fit" function of PyMOL. The DNA duplex from each glycosylase structure was spliced into the histone-bound DNA duplex by creating a new PyMOL object containing bases –72 to –2 and +6 to +72 of strand "I" of the NCP structure, the corresponding complement bases of strand "J" of the NCP structure, and the central 7 base pairs (including the lesion base pair) of the glycosylase duplex. Covalent bonds were added to seal the DNA phosphate backbone. The geometry of each complex was optimized using the built-in energy minimization function of Chimera[17] with 200 steps of steepest-descent minimization followed by 10 steps of conjugate gradient minimization. Incomplete side chains were replaced using the Dunbrack rotamer library.[18] Charges were assigned using AMBER force field ff14SB for standard residues and Antechamber with force field AM1-BCC for nonstandard residues.[19] Following structural optimization, color ramps were applied to surface representations of each glycosylase in PyMOL to generate maps indicating proximity to the histone core.

**PDB Accession Codes**

NCP: 3LZ0
hUNG: 1EMH
hOGG1: 1EBM
Fpg: 1K82
hAAG: 1EWN
EndoIII: 1P59

## SUPPLEMENTAL REFERENCES

(1) Vasudevan, D., Chua, E. Y. D., and Davey, C. A. (2010) Crystal structures of nucleosome core particles containing the "601" strong positioning sequence. *J. Mol. Biol. 403*, 1–10.
(2) Stivers, J. T., Shuman, S., and Mildvan, A. S. (1994) Vaccinia DNA topoisomerase I: single-turnover and steady-state kinetic analysis of the DNA strand cleavage and ligation reactions. *Biochemistry 33*, 327–339.
(3) Zebala, J. A., Choi, J., and Barany, F. (1992) Characterization of steady state, single-turnover, and binding kinetics of the *Taq*I restriction endonuclease. *J. Biol. Chem. 267*, 8097–8105.
(4) Ye, Y., Stahley, M. R., Xu, J., Friedman, J. I., Sun, Y., McKnight, J. N., Gray, J. J., Bowman, G. D., and Stivers, J. T. (2012) Enzymatic excision of uracil residues in nucleosomes depends on the local DNA structure and dynamics. *Biochemistry 51*, 6028–6038.
(5) Maher, R. L., Prasad, A., Rizvanova, O., Wallace, S. S., and Pederson, D. S. (2013) Contribution of DNA unwrapping from histone octamers to the repair of oxidatively damaged DNA in nucleosomes. *DNA Repair 12*, 964–971.
(6) Bellamy, S. R. W., Krusong, K., and Baldwin, G. S. (2007) A rapid reaction analysis of uracil DNA glycosylase indicates an active mechanism of base flipping. *Nucleic Acids Res. 35*, 1478–1487.
(7) Wong, I., Lundquist, A. J., Bernards, A. S., and Mosbaugh, D. W. (2002) Presteady-state analysis of a single catalytic turnover by *Escherichia coli* uracil-DNA glycosylase reveals a "pinch-pull-push" mechanism. *J. Biol. Chem. 277*, 19424–19432.
(8) Jarem, D. A., Wilson, N. R., and Delaney, S. (2009) Structure-dependent DNA damage and repair in a trinucleotide repeat sequence. *Biochemistry 48*, 6655–6663.
(9) Luger, K., Rechsteiner, T. J., and Richmond, T. J. (1999) Preparation of nucleosome core particle from recombinant histones. *Methods Enzymol. 304*, 3–19.
(10) Luger, K., Rechsteiner, T. J., and Richmond, T. J. (1999) Expression and purification of recombinant histones and nucleosome reconstitution. *Meth. Molec. Biol. 119*, 1–16.
(11) Hayes, J. J., Tullius, T. D., and Wolffe, A. P. (1990) The structure of DNA in a nucleosome. *Proc. Natl. Acad. Sci. USA 87*, 7405–7409.
(12) Jain, S. S., and Tullius, T. D. (2008) Footprinting protein–DNA complexes using the hydroxyl radical. *Nat. Protoc. 3*, 1092–1100.
(13) Das, R., Laederach, A., Pearlman, S. M., Herschlag, D., and Altman, R. B. (2005) SAFA: semi-automated footprinting analysis software for high-throughput quantification of nucleic acid footprinting experiments. *RNA 11*, 344–354.
(14) O'Brien, P. J., and Ellenberger, T. E. (2003) Human alkyladenine DNA glycosylase uses acid-base catalysis for selective excision of damaged purines. *Biochemistry 42*, 12418–12429.
(15) Mchugh, P. J., and Knowland, J. (1995) Novel reagents for chemical cleavage at abasic sites and UV photoproducts in DNA. *Nucleic Acids Res. 23*, 1664–1670.
(16) The PyMOL Molecular Graphics System. Schrödinger, LLC.
(17) Pettersen, E. F., Goddard, T. D., Huang, C. C., Couch, G. S., Greenblatt, D. M., Meng, E. C., and Ferrin, T. E. (2004) UCSF Chimera - A visualization system for exploratory research and analysis. *J. Comput. Chem. 25*, 1605–1612.
(18) Dunbrack, R. L. (2002) Rotamer libraries in the 21st century. *Curr. Opin. Struct. Biol. 12*, 431–440.
(19) Wang, J., Wang, W., Kollman, P. A., and Case, D. A. (2006) Automatic atom type and bond type perception in molecular mechanical calculations. *J. Mol. Graph. Model. 25*, 247–260.